

# Variants in Mitochondrial ATP Synthase Cause Variable Neurologic Phenotypes

Michael Zech, MD ,<sup>1,2‡</sup> Robert Kopajtich, MSc ,<sup>1,2‡</sup> Katja Steinbrücker, MD,<sup>3‡</sup>  
 Céline Bris, PhD,<sup>4,5</sup> Naig Gueguen, PhD,<sup>4,5</sup> René G. Feichtinger, PhD ,<sup>3</sup>  
 Melanie T. Achleitner, MSc,<sup>3</sup> Neslihan Duzkale, MD,<sup>6</sup> Maximilien Pérvier, MD,<sup>7</sup>  
 Johannes Koch, MD,<sup>3</sup> Harald Engelhardt, MD,<sup>8</sup> Peter Freisinger, MD,<sup>9</sup>  
 Matias Wagner, MD ,<sup>1,2</sup> Theresa Brunet, MD ,<sup>1,2</sup> Riccardo Berutti, PhD,<sup>1,2</sup>  
 Dmitrii Smirnov, MSc ,<sup>1,2</sup> Tharsini Navaratnarajah, MSc,<sup>10</sup> Richard J.T. Rodenburg, PhD,<sup>11</sup>  
 Lynn S Pais, MS,<sup>12</sup> Christina Austin-Tse, PhD,<sup>13</sup> Melanie O'Leary, MS,<sup>14</sup> Sylvia Boesch, MD,<sup>15</sup>  
 Robert Jech, MD,<sup>16</sup> Somayeh Bakhtiari, PhD,<sup>17,18</sup> Sheng Chih Jin, PhD,<sup>19,20</sup>  
 Friederike Wilbert, MD,<sup>21</sup> Michael C Kruer, MD,<sup>17,18</sup> Saskia B. Wortmann, MD,<sup>3,22</sup>  
 Matthias Eckenweiler, MD,<sup>21</sup> Johannes A. Mayr, MD,<sup>3</sup> Felix Distelmaier, MD,<sup>10</sup>  
 Robert Steinfeld, MD,<sup>23</sup> Juliane Winkelmann, MD,<sup>1,2,24,25†</sup> and Holger Prokisch, PhD <sup>1,2†</sup>

View this article online at [wileyonlinelibrary.com](https://onlinelibrary.wiley.com/doi/10.1002/ana.26293). DOI: 10.1002/ana.26293

Received Aug 23, 2021, and in revised form Dec 23, 2021. Accepted for publication Dec 24, 2021.

Address correspondence to Dr Zech, Institute of Neurogenomics, Helmholtz Zentrum München, Deutsches Forschungszentrum für Gesundheit und Umwelt (GmbH), Ingolstädter Landstraße 1, 85764 Neuherberg, Germany. E-mail: michael.zech@mri.tum.de Dr Holger Prokisch, Institute of Neurogenomics, Helmholtz Zentrum München, Deutsches Forschungszentrum für Gesundheit und Umwelt (GmbH), Ingolstädter Landstraße 1, 85764 Neuherberg, Germany. E-mail: prokisch@helmholtz-muenchen.de

<sup>‡</sup>These authors contributed equally to this work as first authors.

<sup>†</sup>These authors contributed equally to this work as last authors.

From the <sup>1</sup>Technical University of Munich, School of Medicine, Institute of Human Genetics, Munich, Germany; <sup>2</sup>Institute of Neurogenomics, Helmholtz Zentrum München, Munich, Germany; <sup>3</sup>University Children's Hospital, Paracelsus Medical University (PMU), Salzburg, Austria; <sup>4</sup>Unité Mixte de Recherche MITOVASC, CNRS 6015/INSERM 1083, Université d'Angers, Angers, France; <sup>5</sup>Département de Biochimie et Génétique, Centre Hospitalier Universitaire d'Angers, Angers, France; <sup>6</sup>Department of Medical Genetic, Diskapi Yildirim Beyazit Training and Research Hospital, Ankara, Turkey; <sup>7</sup>Pediatric Neurology Department, CHU Clocheville, Tours, France; <sup>8</sup>Kinderkrankenhaus St. Marien gGmbH, Zentrum für Kinder- und Jugendmedizin, Landshut, Germany; <sup>9</sup>Children's Hospital Kreiskliniken, Reutlingen, Germany; <sup>10</sup>Department of General Pediatrics, Neonatology and Pediatric Cardiology, University Children's Hospital, Medical Faculty, Heinrich-Heine-University, Düsseldorf, Germany; <sup>11</sup>Radboud Centre for Mitochondrial Medicine, Department of Paediatrics Radboud Institute for Molecular Life Sciences, Radboud University Nijmegen Medical Centre Nijmegen, Nijmegen, The Netherlands; <sup>12</sup>Program in Medical and Population Genetics, Broad Institute, Cambridge, MA; <sup>13</sup>Harvard Medical School & Center for Genomic Medicine, Massachusetts General Hospital, Boston & Laboratory for Molecular Medicine, Partners Healthcare Personalized Medicine, Cambridge, MA; <sup>14</sup>Broad Center for Mendelian Genomics, Broad Institute of MIT and Harvard, Cambridge, MA; <sup>15</sup>Department of Neurology, Medical University of Innsbruck, Innsbruck, Austria; <sup>16</sup>Department of Neurology, Charles University, 1st Faculty of Medicine and General University Hospital in Prague, Prague, Czech Republic; <sup>17</sup>Pediatric Movement Disorders Program, Division of Pediatric Neurology, Barrow Neurological Institute, Phoenix Children's Hospital, Phoenix, AZ; <sup>18</sup>Departments of Child Health, Neurology, and Cellular & Molecular Medicine, and Program in Genetics, University of Arizona College of Medicine-Phoenix, Phoenix, AZ; <sup>19</sup>Department of Genetics, Washington University School of Medicine, St. Louis, MO; <sup>20</sup>Department of Pediatrics, Washington University School of Medicine, St. Louis, MO; <sup>21</sup>Department of Neuropediatrics and Muscle Disorders, University Medical Center, Faculty of Medicine, University of Freiburg, Freiburg, Germany; <sup>22</sup>Radboud Center for Mitochondrial Medicine, Department of Pediatrics, Amalia Children's Hospital, Radboud UMC, Nijmegen, The Netherlands; <sup>23</sup>Department of Pediatric Neurology, University Children's Hospital Zurich, University of Zurich, Zurich, Switzerland; <sup>24</sup>Lehrstuhl für Neurogenetik, Technische Universität München, Munich, Germany; and <sup>25</sup>Munich Cluster for Systems Neurology (SyNergy), Munich, Germany

Additional supporting information can be found in the online version of this article.

**Objective:** ATP synthase (ATPase) is responsible for the majority of ATP production. Nevertheless, disease phenotypes associated with mutations in ATPase subunits are extremely rare. We aimed at expanding the spectrum of ATPase-related diseases.

**Methods:** Whole-exome sequencing in cohorts with 2,962 patients diagnosed with mitochondrial disease and/or dystonia and international collaboration were used to identify deleterious variants in ATPase-encoding genes. Findings were complemented by transcriptional and proteomic profiling of patient fibroblasts. ATPase integrity and activity were assayed using cells and tissues from 5 patients.

**Results:** We present 10 total individuals with biallelic or de novo monoallelic variants in nuclear ATPase subunit genes. Three unrelated patients showed the same homozygous missense *ATP5F1E* mutation (including one published case). An intronic splice-disrupting alteration in compound heterozygosity with a nonsense variant in *ATP5PO* was found in one patient. Three patients had de novo heterozygous missense variants in *ATP5F1A*, whereas another 3 were heterozygous for *ATP5MC3* de novo missense changes. Bioinformatics methods and populational data supported the variants' pathogenicity. Immunohistochemistry, proteomics, and/or immunoblotting revealed significantly reduced ATPase amounts in association to *ATP5F1E* and *ATP5PO* mutations. Diminished activity and/or defective assembly of ATPase was demonstrated by enzymatic assays and/or immunoblotting in patient samples bearing *ATP5F1A*-p.Arg207His, *ATP5MC3*-p.Gly79Val, and *ATP5MC3*-p.Asn106Lys. The associated clinical profiles were heterogeneous, ranging from hypotonia with spontaneous resolution (1/10) to epilepsy with early death (1/10) or variable persistent abnormalities, including movement disorders, developmental delay, intellectual disability, hyperlactatemia, and other neurologic and systemic features. Although potentially reflecting an ascertainment bias, dystonia was common (7/10).

**Interpretation:** Our results establish evidence for a previously unrecognized role of ATPase nuclear-gene defects in phenotypes characterized by neurodevelopmental and neurodegenerative features.

ANN NEUROL 2022;91:225–237

The primary means of producing ATP for eukaryotic cells is oxidative phosphorylation (OXPHOS), which takes place in mitochondria.<sup>1</sup> OXPHOS is carried out by 5 multi-subunit complexes, 4 of which (respiratory chain complexes I–IV) work in concert to create a transmembrane electrochemical ion gradient.<sup>1</sup> The fifth complex, ATP synthase (ATPase), also known as  $F_0/F_1$ -ATPase or complex V, uses the electrochemical energy provided by the respiratory chain to synthesize ATP from ADP.<sup>2</sup> Encoded by 17 nuclear and 2 mitochondrial genes,<sup>3</sup> ATPase is

composed of 2 distinct, but physically linked components: the  $F_0$  part is a membrane-embedded ion-translocating channel and contains 12 subunits (a–g, i, k, F6, OSCP, and A6L) whereas  $F_1$  (containing subunits  $\alpha_3\beta_3\gamma\delta\epsilon$ ) is the catalytic core where ATP generation occurs (Fig 1).<sup>4</sup> Despite the essential function of ATPase, mutational defects of its subunit genes have rarely been implicated in human disorders.<sup>5,6</sup> Most cases of ATPase-related disease have been attributed to variants in the mitochondrial gene-encoded subunits a (*MT-ATP6*) and A6L (*MT-ATP8*), causing a spectrum of

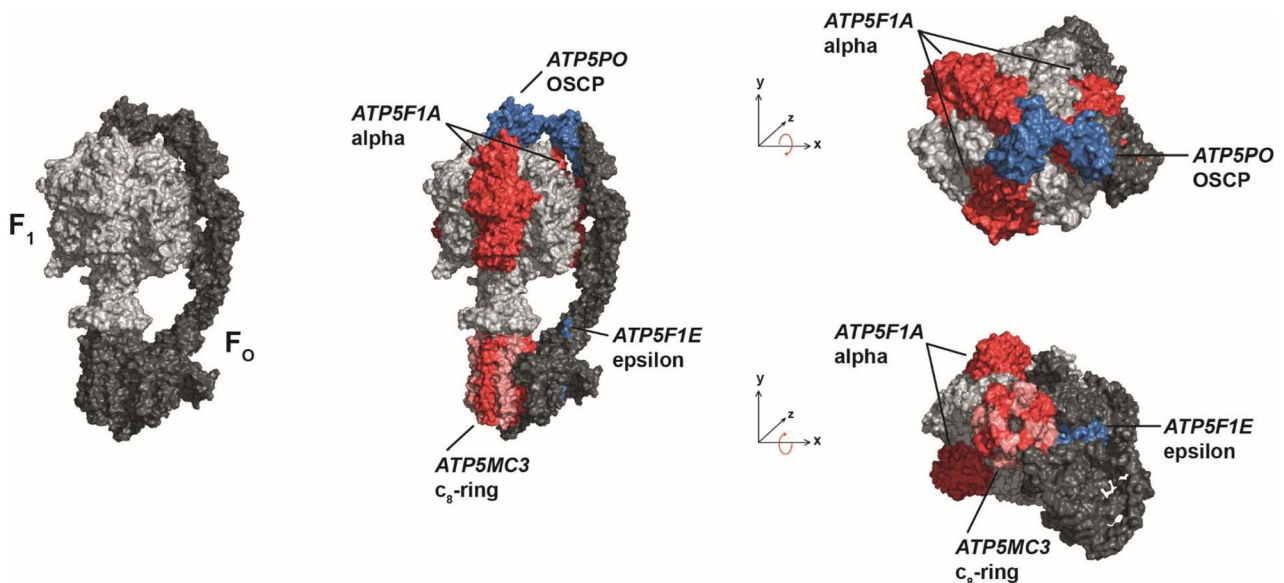


**FIGURE 1:** Schematic views illustrating the subunits of mitochondrial ATPase mutated in patients of this study. ATPase consists of 2 functional domains,  $F_0$  (dark gray) and  $F_1$  (light gray). Variant-bearing subunits are shown in red and blue colors:  $\epsilon$ -subunit (encoded by *ATP5F1E*); OSCP-subunit (encoded by *ATP5PO*);  $\alpha$ -subunit (encoded by *ATP5F1A*); and subunit c (encoded by *ATP5MC3*).

conditions, including neurogenic-muscle-weakness, ataxia, and retinitis-pigmentosa (NARP) syndrome, familial bilateral striatal necrosis, Leigh syndrome, and neuropathy-cardiomyopathy phenotypes (MIM:516060/516070).<sup>6,7</sup> By contrast, only 10 families with disease-associated mutations in nuclear genes coding for ATPase subunits have been described.<sup>6,8</sup> In 2010, our group reported a specific *ATP5F1E* homozygous variant in a single patient with neuropathy, intellectual disability, and ataxia (MIM:614053),<sup>9</sup> but this association has not been firmly established. Autosomal-recessively inherited mutations were subsequently identified in *ATP5F1A* in 2 families with lethal infantile encephalopathy (MIM:615228/616045)<sup>10,11</sup>; in *ATP5F1D* in 2 families with metabolic encephalopathic crises (MIM:618120)<sup>12</sup>; and in *ATP5MK* in 3 families with Leigh syndrome (MIM:615204).<sup>13</sup> Very recently, our group has contributed to the delineation of a movement-disorder syndrome caused by an autosomal-dominant recurrent variant in *ATP5MC3*<sup>8</sup>; 2 independent families have been reported, including one with a single affected patient who was also part of the present study cohort. However, no biochemical cellular phenotype has yet been defined for this latter individual, leaving the patient's characterization incomplete in the previous publication.<sup>8</sup> Moreover, because only one mutant genotype has been documented, additional clinical and molecular observations remain necessary to confirm *ATP5MC3* as a Mendelian-disease locus.

Herein, through multicenter collaboration and community data-sharing, we gathered a series of 10 nonrelated patients harboring either biallelic or de novo monoallelic variants in 4 distinct nuclear-DNA-encoded ATPase subunits. We provide functional and in silico evidence to support the causative nature of homozygous variants in *ATP5F1E* (3 cases), compound-heterozygous variants in *ATP5PO* (1 case), and heterozygous variants in *ATP5F1A* and *ATP5MC3* (3 cases each). The observed phenotypes establish a range of neurodevelopmental and neurodegenerative symptoms in association to ATPase deleterious variation, including prominent movement-disorder/dystonia manifestations. By including 2 previously published patients (with extended data), we are able to provide prevalence estimates for ATPase-related disorders in large mitochondrial-disease and dystonia cohorts and characterize pheno-genotypically a broad set of affected families. Our analysis identifies de novo mutational events as a more generalizable mechanism in mitochondrial-disease genetics and begins to describe a relationship between the extent of ATPase dysfunction and clinical severity.

## Subjects and Methods

### Patient Ascertainment

Two large patient collections were used as the cohorts for initial analysis in this study. The first cohort comprised 1,950 whole-

exome-sequenced individuals with suspected mitochondrial defect syndromes, for whom data had been collected in the frame of our research program GENOMIT.<sup>14</sup> The second cohort included 1,012 patients with dystonia-affected syndromes with whole-exome sequencing (WES) data (Munich, Germany).<sup>15</sup> Patients in both cohorts had been recruited via European collaborative networks with previously described enrollment criteria.<sup>14,15</sup> Patients 1, 2, 4, 5, and 9 were found in the GENOMIT database; Patients 6 and 8 were identified from the dystonia cohort. Communications between collaborators and GeneMatcher postings<sup>16</sup> facilitated the identification of additional cases. These subjects were enrolled in the following centers investigating the causes of rare neurologic diseases: Diskapi-Yildirim-Beyazit-Hospital of Ankara (Turkey; Patient 3); Phoenix Children's Hospital and Broad Center for Mendelian Genomics (USA; Patient 7); and University-Hospital-Center (CHU) of Tours (France; Patient 10). All patients presented in this work had unremarkable standard genetic screenings as part of local clinical assessments; metabolic studies documented elevated lactate levels for 7 cases and abnormal organic acids for 3 cases. Phenotype data collection involved a detailed review of medical histories, routine diagnostic findings, and current neurologic examinations. Written informed consent was obtained from all study participants or their legal caretakers according to institutional ethics committees' policies.

### Variant Prioritization

In the initial analysis, WES data from participants of the GENOMIT and dystonia studies were searched for potentially deleterious variants in ATPase subunit genes (as summarized by He et al<sup>3</sup>), excepting the well-established mitochondrially encoded disease genes *MT-ATP6* and *MT-ATP8*. Variants in the set of 17 genes were prioritized on the basis of their effect on amino-acid sequence, frequency within general population databases (gnomAD, internal exomes) using thresholds of 0.01% for autosomal-dominant/X-linked variants and 0.5% for autosomal-recessive variants, position in a conserved genomic interval, in silico deleteriousness predictions, and described pathological impact. Priority was given to rare, non-synonymous and splice-region variants fitting a recessive (homozygous or compound heterozygous) or a de novo dominant model. Discoveries were shared with collaborating researchers who independently determined candidate variants in *ATP5F1E*, *ATP5F1A*, and *ATP5MC3* following their in-house pipelines.

### Whole-Exome and Sanger Sequencing

Ten patients with ATPase variants had undergone WES according to previously reported methodologies.<sup>14,15,17–19</sup> Briefly, target enrichment for 2,962 affected individuals in the GENOMIT and dystonia studies was performed with Agilent SureSelect equipment at Helmholtz-Center-Munich (Munich, Germany; >90% of samples) and 4 other institutions connected to these research initiatives. Library DNA was sequenced on Illumina high-throughput systems in 100-bp paired-end mode. Samples achieved an average depth-of-coverage of  $\geq 50$  times. Reads were aligned to human genome-build GRCh37/hg19 and

assessed for sequence alterations using a custom-made bioinformatics tool.<sup>14,15</sup> For Patients 3, 7, and 10, identified by communication with additional laboratories, WES was carried out with target-enrichment designs according to the manufacturers' specifications.<sup>17–19</sup> Sequencing and downstream analyses were performed using published platforms and pipelines.<sup>17–19</sup> All prioritized variants were verified by Sanger sequencing.

### **In Silico Analysis**

ATPase-protein sequences were obtained from Uniprot<sup>20</sup> and Clustal-Omega<sup>21</sup> was used to assess conservation of amino-acids across species. Missense-variant pathogenicity prediction was done with SIFT, PolyPhen2, and CADD.<sup>22–24</sup> The PDB<sup>25</sup> macromolecule 6ZQM, containing bovine ATPase crystal structures with strong identity to human ATPase (>95%), was used for modeling analyses; proteins were visualized with PyMol (Schrödinger).

### **Cell Culture**

Skin-derived fibroblasts of Patients 2, 4, 8, and 10 were cultured as described previously.<sup>26,27</sup> Skin fibroblasts from healthy donors and a *KARS*-mutated individual were used as control lines.

### **Fluorescence Staining of Fibroblasts**

Fibroblasts of Patient 2 and 6 controls were fixated overnight in a 4% formaldehyde solution at 4°C.<sup>9,26</sup> Samples were washed with phosphate buffered saline with 0.5% Tween-20 (PBS-T). Antigen retrieval was performed in 1 mM EDTA, 0.05% Tween-20, pH 8 for 40 minutes at 95°C. Samples were allowed to cool down to room temperature (RT) for 20 minutes. After additional washes with PBS-T, the following antibody dilutions were used: VDAC1 (1:400), NDUFS4 (1:100), SDHA (1:400), UQCRC2 (1:400), MT-CO1 (1:100), and ATP5F1A (1:400). Primary antibodies were diluted in DAKO antibody diluent and slides were incubated for 1 hour at RT. Samples were washed with PBS-T and incubated with anti-mouse Alexa Fluor-488 (1:500) and anti-rabbit Alexa Fluor-594 (1:1000) in PBS-T for 1 hour at RT. Slides were washed with PBS-T and incubated 10 minutes with DAPI 1:2000 in PBS-T. Samples were washed twice in ddH<sub>2</sub>O and mounted in Fluorescence Mounting Media (DAKO).

### **Fluorescence Staining of Blood Smears**

Blood smears of Patient 2 and 2 controls were air-dried at RT. Slides were fixated overnight in a 4% formaldehyde solution at 4°C. Samples were washed with PBS-T. Antigen retrieval was performed in 1 mM EDTA, 0.05% Tween-20, pH 8 for 20 minutes at 95°C. Samples were allowed to cool down to RT for 20 minutes and washed with PBS-T. Anti-ATP5F1A (1:400) and anti-VDAC1 (1:400) were diluted in DAKO antibody diluent and slides were incubated for 1 hour at RT. Samples were washed with PBS-T and incubated with anti-mouse Alexa Fluor-488 (1:500) and anti-rabbit Alexa Fluor-594 (1:1000) in PBS-T for 1 hour at RT. Slides were washed with PBS-T and incubated 10 minutes with DAPI 1:2000 in PBS-T. Samples were washed

twice in ddH<sub>2</sub>O and mounted in Fluorescence Mounting Media (DAKO).

### **Oxygen Consumption Rate Measurement**

Oxygen consumption rate (OCR) measurement was done in the fibroblasts of Patients 2 and 8 and 2 controls with a XF96 Extracellular Flux Analyzer (Seahorse, Agilent). Sample preparation was performed as previously described and reaction runs were undertaken using established conditions.<sup>26</sup> Recordings were also performed with the addition of carbonyl cyanide 4-(trifluoromethoxy) phenylhydrazone (FCCP).<sup>26</sup>

### **RNA-Sequencing**

Fibroblasts of Patient 4 were subjected to strand-specific, polyA-enriched RNA-seq according to published protocols.<sup>28</sup> Following RNA-integrity assessment (BioAnalyzer), libraries were prepared as described in the TruSeq Stranded mRNA Sample Prep Guide (Illumina) and sequenced as 100-bp paired-end runs on a NovaSeq6000. Reads were mapped to GRCh37/hg19 using STAR-aligner. *ATP5PO* mRNA levels were assessed by comparing FPKM values in a cohort of 317 samples. Aberrant splicing events were manually inspected using the Integrative Genomics Viewer.

### **Quantitative Proteomics**

Quantitative tandem mass tag (TMT) proteomics on fibroblast material from Patient 4 was performed using previously described sample preparation and data-analysis methods.<sup>29,30</sup> Patient fibroblasts were analyzed in a TMT-batch of 8 cell lines. Identification of expression outliers was computed by comparing one sample against all others in a moderated *t* test approach using the R/Bioconductor package *limma*.<sup>31</sup>

### **Blue Native Gel Electrophoresis**

Fibroblasts of Patients 4 and 10 as well as 10 controls were harvested with TrypLE Select (Gibco/Life Technologies) and washed twice with ice-cold PBS.<sup>26</sup> For mitoplast fraction, cell pellets were treated with 2 mg/ml digitonin in PBS for 10 minutes on ice. Mitoplast fractions were pelleted and washed twice with PBS. OXPHOS enzymes were isolated by treatment with 2% *n*-dodecyl- $\beta$ -maltoside supplemented with 10  $\mu$ l/ml protease inhibitor cocktail and 1 mM PMSF (Sigma Aldrich) for 10 minutes on ice and subsequent centrifugation. For blue native gel electrophoresis (BN-PAGE), protein extracts were separated on 3 to 18% gradient gels. Protein bands were transferred onto polyvinylidene difluoride (PVDF) membranes using a Trans-Blot SD semi-dry transfer cell (Bio-Rad). Membranes were decorated with antibodies against the following mitochondrial proteins: anti-ATP5F1A; anti-NDUFS3; anti-ATP5F1B; and anti-SDHA.

### **Enzyme Activity Assays**

OXPHOS enzyme and citrate synthase activities in muscle tissue (Patient 5) or fibroblasts (Patients 8 and 10) were assessed spectrophotometrically using standard procedures.<sup>26,27,32</sup> Thirty-seven and 100 internal control samples were used in the experiments with muscle and fibroblasts, respectively. The mitochondrial fraction of

muscle crude homogenates<sup>26</sup> or fibroblast cultures<sup>27,32</sup> was subjected to activity measurements.

## Results

Analysis of 2,962 GENOMIT and dystonia study exomes<sup>14,15</sup> in combination with gene matching<sup>16</sup> led to identification of 10 independent individuals bearing novel or rare, probably deleterious variants in ATPase genes as the most plausible candidates; the affected subunits within the

ATPase complex are illustrated in Figure 1. We observed a recurrent homozygous variant in *ATP5F1E*, 2 compound-heterozygous variants in *ATP5PO*, and 6 different de novo variants in *ATP5F1E* and *ATP5MC3* (Table). There was phenotypic heterogeneity in the patients, with a range of features encompassing early onset dystonia, spasticity, ataxia, metabolic disturbances with lactic acidosis, seizures, neuro-pathic signs, and neurodevelopmental impairment of varying degree. Supplementary Table S1 summarizes the clinical

**TABLE. Identified ATPase Gene Variants**

Patient	Gene; Encoded protein	RefSeq annotations	Variants(s) (cDNA, protein)	Zygoty	In silico pathogenicity predictions (CADD; PolyPhen2; SIFT)	ACMG classification (pathogenic/likely pathogenic)
1	<i>ATP5F1E</i> ; ATP synthase subunit epsilon, mitochondrial	NM_006886.4; NP_008817.1	c.35A > G, p. Tyr12Cys	homozygous	26.1; 1.0 (probably damaging); 0	PS3, PS4_moderate, PM2, PP3
2			c.35A > G, p. Tyr12Cys	homozygous	26.1; 1.0 (probably damaging); 0	PS3, PS4_moderate, PM2, PP3
3			c.35A > G, p. Tyr12Cys	homozygous	26.1; 1.0 (probably damaging); 0	PS3, PS4_moderate, PM2, PP3
4	<i>ATP5PO</i> ; ATP synthase subunit O, mitochondrial	NM_001697.3; NP_001688.1	c.34C > T, p. Gln12*; c.329-20A > G	compound heterozygous	c.34C > T: 36; N/A; c.329-20A > G: 2.323; N/A; N/A	PS3, PM2
5	<i>ATP5F1A</i> ; ATP synthase subunit alpha, mitochondrial	NM_004046.6; NP_004037.1	c.620G > A, p. Arg207His	heterozygous, de novo	35; 0.999 (probably damaging); 0.01	PS2, PS3, PM2, PP3
6			c.545G > A, p. Arg182Gln	heterozygous, de novo	34; 0.692 (possibly damaging); 0.01	PS2, PM2, PP3
7			c.1037C > T, p.Ser346Phe	heterozygous, de novo	32; 1.0 (probably damaging); 0	PS2, PM2, PP3
8	<i>ATP5MC3</i> ; ATP synthase F(0) complex subunit C3, mitochondrial	NM_001689.5; NP_001680.1	c.318C > G, p.Asn106Lys	heterozygous, de novo	26.1; 1.0 (probably damaging); 0	PS2, PS3, PS4_moderate, PM2, PP3
9			c.319C > G, p.Pro107Ala	heterozygous, de novo	24.1; 0.931 (probably damaging); 0	PM2, PM6, PP2, PP3
10			c.236G > T, p.Gly79Val	heterozygous, de novo	34; 0.907 (possibly damaging); 0	PS2, PS3, PM2, PP3

ACMG = American College of Medical Genetics & Genomics; N/A = not available.

findings of each subject; long-term follow-up is provided for Patient 1, who was previously published in a single-case study<sup>9</sup>; Patient 8 has been part of a very recent targeted assessment of a certain recurrent *ATP5MC3* variant,<sup>8</sup> but no functional studies of this individual's primary cells have been published before.

### ATP5F1E Variants

Three individuals (Patients 1, 2, and 3) with biallelic variants in *ATP5F1E* were identified (Fig 2A). In these patients, the same homozygous c.35A > G (p.Tyr12Cys) missense variant was found, whereas their unaffected parents were heterozygous for the mutation. The variant, unobserved in controls, was previously shown by us to result in ATPase deficiency with diminished OXPHOS capacity in Patient 1's cells.<sup>9</sup> In support of these findings, fluorescence staining of OXPHOS proteins in fibroblasts from Patient 2 revealed markedly decreased amounts of the ATPase marker ATP5F1A relative to controls (Fig 2B). Additionally, a staining assay to detect ATPase components in blood smears showed that ATP5F1A levels were not

detectable in Patient 2's leukocytes and thrombocytes (Fig 2C). The OCR of Patient 2 was significantly reduced relative to a control individual (Fig 2D). In assessments of Patient 1's long-term clinical outcome (11-year period since the original description, 33 years old), we observed a non-progressive disease course with intellectual disability, ataxia, and axonal-demyelinating polyneuropathy; she had developed gait impairment with limb dystonia. Episodes of infection-triggered metabolic deterioration, observed in her first years of life,<sup>9</sup> had resolved. Patient 2, a 16-month-old infant, presented after birth with vomiting, severe respiratory distress, seizures, and impaired consciousness associated with lactic acidosis. Metabolic abnormalities improved spontaneously, but she experienced development delay and progressively developed generalized dystonia with poor response to trialed medications; she also had visual and hearing deficits. Patient 3, a 13-year-old girl, was evaluated for intellectual disability, gait ataxia, and peripheral neuropathy. During infancy, she manifested lactic acidosis with transient respiratory failure, developmental delay, and episodes of generalized tonic-clonic seizures.

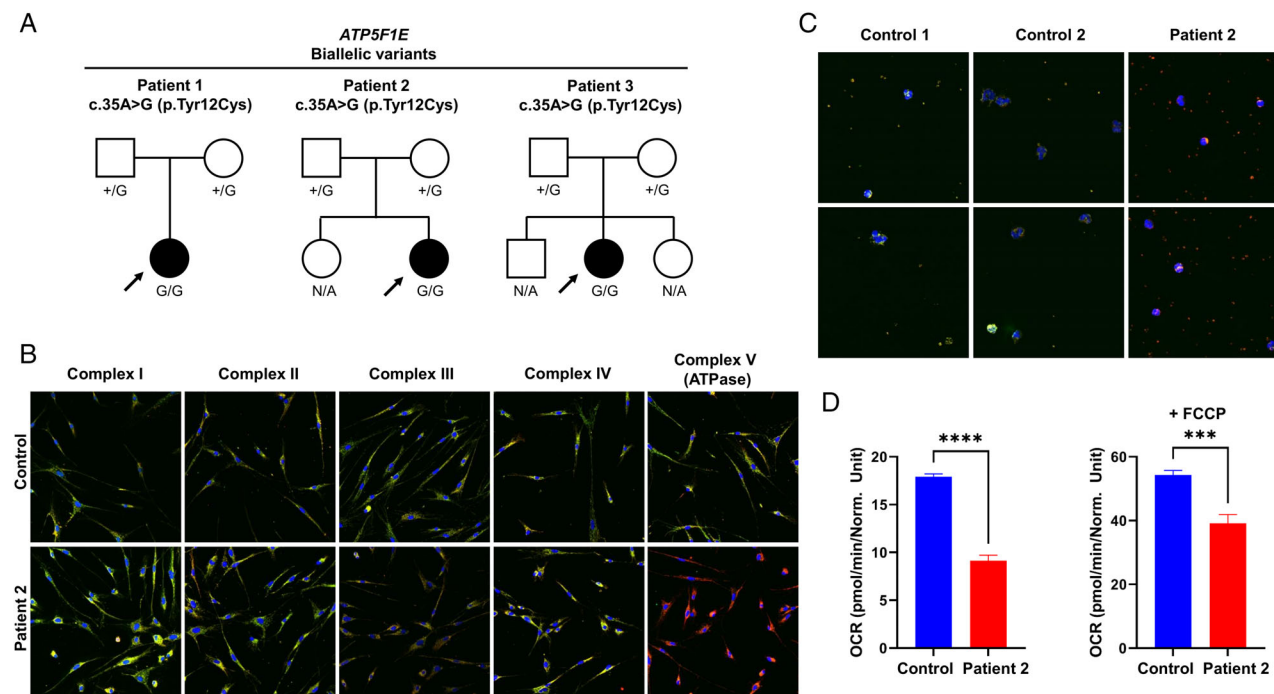


**FIGURE 2:** Biallelic *ATP5F1E* variants identified in 3 cases. (A) Pedigree drawings for 3 families with the homozygous variant in *ATP5F1E*. N/A, no genotyping available. (B) Fluorescence staining of Patient 2's primary human skin fibroblasts and a fibroblast control line. Cells were stained with antibodies raised against subunits of the 5 OXPHOS complexes (green) and an antibody against VDAC1 (red). The merge is shown. A shift to red indicates a reduction of the respective OXPHOS subunit. The images were taken with a 200 times magnification. The experiment was performed with analysis of 6 different control lines (data not shown) and repeated twice with similar results. (C) Fluorescence staining of blood smears from Patient 2 and 2 different control lines. Cells were stained with an antibody raised against the ATP5F1A subunit of ATPase (green) and an antibody against VDAC1 (red). The merge is shown. A shift to red indicates a reduction of the ATP5F1A subunit. The images were taken with a 400 times magnification. The experiment was repeated twice with similar results. (D) Measurement of oxygen consumption rate (OCR) in Patient 2's fibroblasts and a control line. Data show the mean values  $\pm$  SEM of basal respiration (left graph) and of maximal respiration after addition of FCCP (right graph); number of replicates: Patient = 4; control = 8; \*\*\*\*p < 0.0001, \*\*\*p < 0.001. OXPHOS = oxidative phosphorylation.

**ATP5PO Variants**

One individual (Patient 4) was found to have biallelic, compound-heterozygous variants in *ATP5PO*: a maternally inherited c.34C > T (p.Gln12\*) nonsense variant;

and a paternally inherited extended splice-site mutation, c.329-20A > G (Fig 3A). The c.34C > T variant was listed 4 times in gnomAD in the heterozygous state, whereas c.329-20A > G was absent from available control

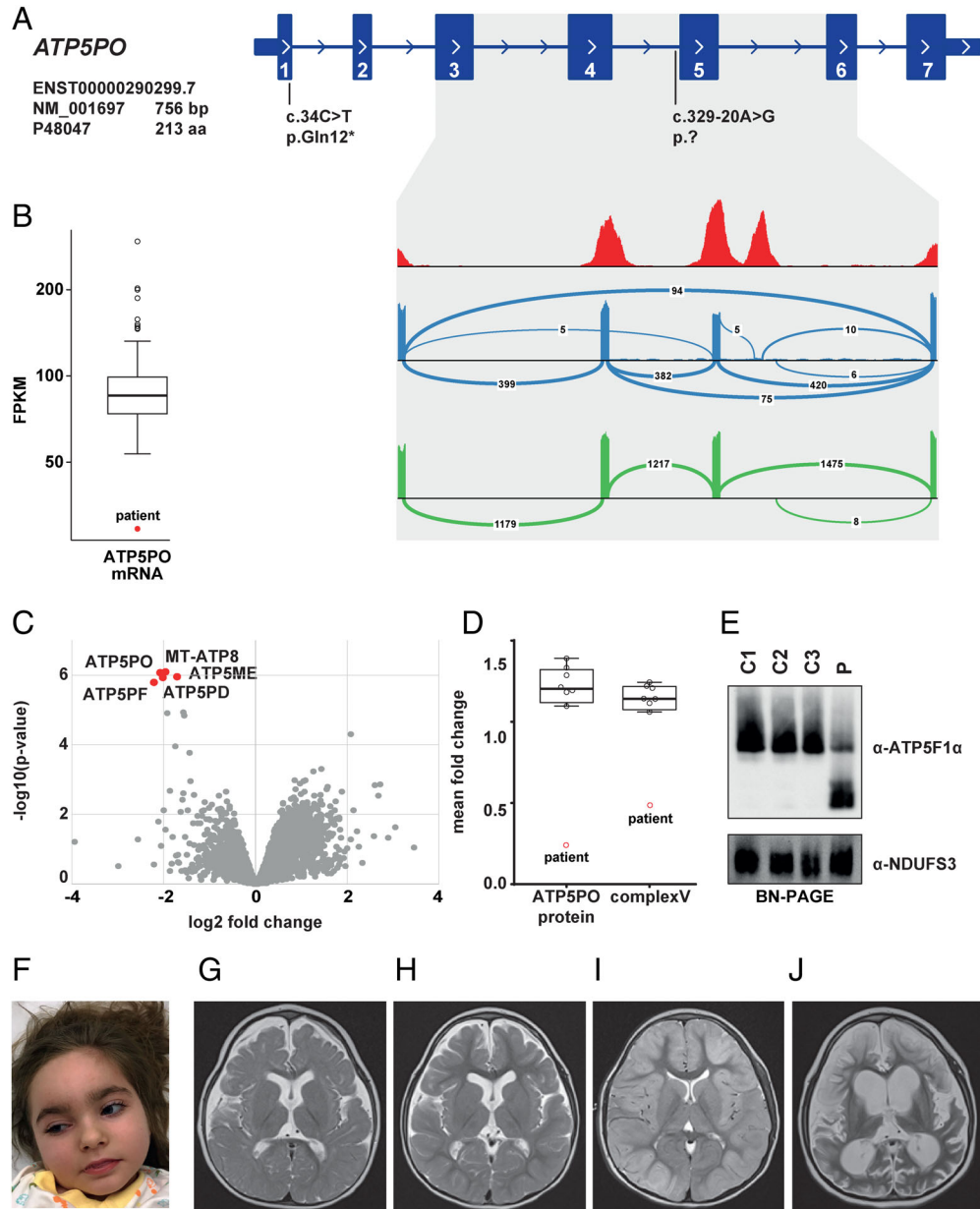


**FIGURE 3:** Biallelic *ATP5PO* variants identified in 1 case. (A) RNA-seq-based detection of a splice defect induced by the intronic variant c.329-20A > G. Sashimi plots to visualize splice junctions demonstrate that the c.329-20A > G allele causes skipping of exon 5 and exons 4 plus 5 (blue graph), resulting in reduced total amounts of *ATP5PO* mRNA levels (B). Wild-type *ATP5PO* produces only the normal transcript (green graph). (C) Proteomic analysis of patient-derived fibroblasts shows significant downregulation of 5 ATPase subunits (red dots) relative to controls. (D) Mass spectrometry-based protein quantification demonstrates a decrease of *ATP5PO* protein and the ATPase holoenzyme. (E) BN-PAGE analysis confirming reduced levels of intact ATPase in Patient 4 (p) relative to 3 different control subjects (C1–C3). The experiment was repeated 3 times with similar results. (F) Clinical photograph of Patient 4 at the age of 5 years. Parental consent was obtained for inclusion of the identifiable (non-obscured) facial photograph shown in this figure. (G–J) Selected MRI brain images for Patient 4; (G) axial T2 image (aged 1 years and 3 months) showing moderately reduced brain volume and delayed myelination. In addition, hypoplasia of the lower part of the cerebellar vermis was noted (not shown); (H) axial T2 image (aged 3 years and 10 months) showing stable findings; (i) axial T2 image (aged 5 years, following a prolonged status epilepticus) showing cortical hyperintensity and diffuse tissue swelling; (j) axial T2 image (aged 5 years and 3 months) showing massive global brain atrophy and tissue defects. BN-PAGE = blue native gel electrophoresis; MRI = magnetic resonance imaging.

databases. RNA-seq performed on patient fibroblasts showed that c.329-20A > G led to skipping of exon 5 and exons 4 plus 5, indicating that this variant was a loss-of-function allele associated with abnormal gene splicing and reduced *ATP5PO* mRNA levels (see Figs 3A, 3B). To gain insight into the molecular consequences of the variants, quantitative proteomic analysis of fibroblasts from the patient relative to independent control samples was performed. We observed significant underexpression of *ATP5PO* and 4 other ATPase subunits in the patient's cell line (see Fig 3C), in addition to a pathologically low overall abundance of ATPase (50%) in this subject (see Fig 3D). BN-PAGE analysis confirmed these results, demonstrating defective ATPase assembly, whereas OXPHOS complex I was not altered (see Fig 3E). The phenotype of this patient, a 6-year-old girl (see Fig 3F), was suggestive of a mitochondrial disease: she presented during the neonatal period with fever-induced partial seizures, hypotonia, and elevated cerebrospinal fluid (CSF) lactate concentrations; examination at 2 years of age revealed acquired

microcephaly, global developmental delay, and dystonia. Magnetic resonance imaging (MRI) studies documented progressive brain atrophy (Figs 3G–J). Following a period of initial stabilization, she developed seizure deterioration and died after several episodes with super-refractory status epilepticus at the age of 6 years.

**ATP5F1A Variants**

Three individuals (Patients 5, 6, and 7) were identified as each having a de novo monoallelic missense variant in *ATP5F1A* (Figs 4A, B). The first individual (Patient 5) was a 14-year-old girl who carried the variant c.620G > A (p.Arg207His). She presented during the first few months of life with developmental delay, failure-to-thrive, and lactic acidosis; subsequently, she recovered and had no persistent neurologic phenotype. The second individual (Patient 6), a 17-year-old boy, harbored a c.545G > A (p.Arg182Gln) variant. He demonstrated psychomotor delay, intellectual disability, ataxia, spastic paraparesis, and dystonia. The last individual (Patient 7), a 12-year-old girl, was

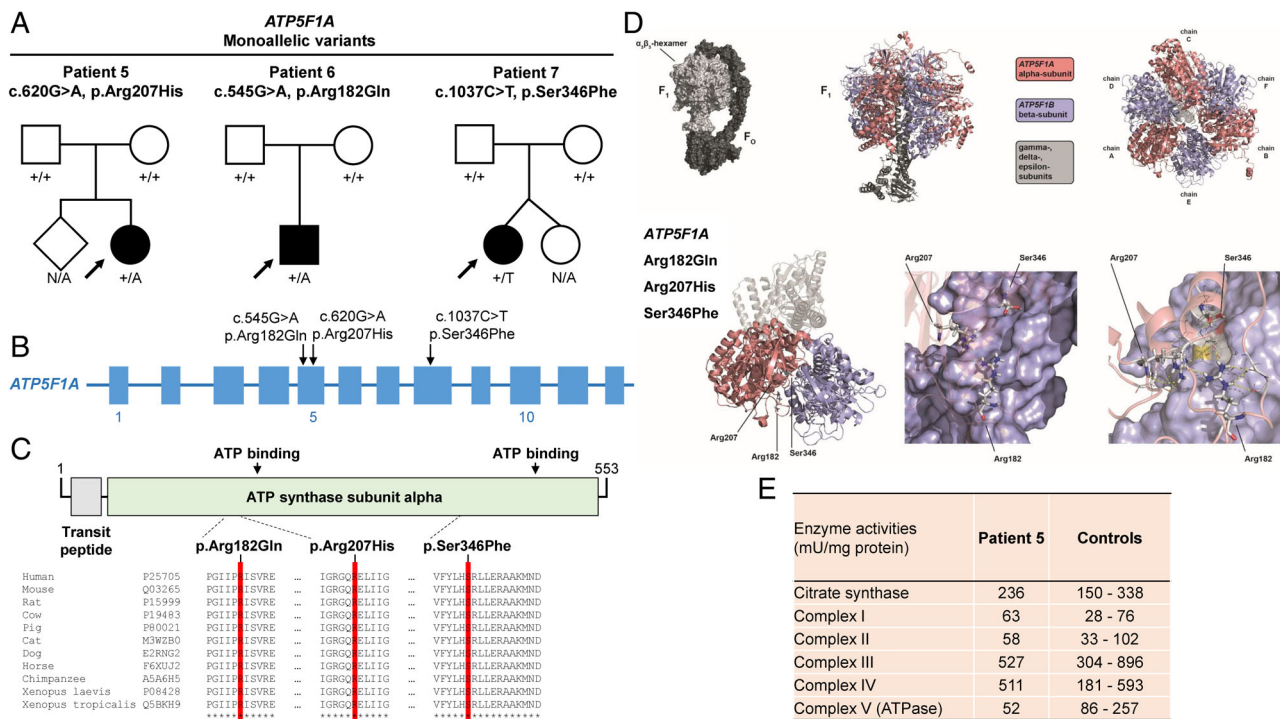


**FIGURE 4:** De novo monoallelic *ATP5F1A* variants identified in 3 cases. (A) Pedigree drawings for 3 families with heterozygous de novo variants in *ATP5F1A*. N/A, no genotyping available. (B) Exon-intron structure of *ATP5F1A* (not drawn to exact scale) with indication of the localizations of identified mutations. (C) Schematic overview of the *ATP5F1A* protein, its domain organization (boundaries are based on UniProt entry P25705), and the protein variants. A multispecies sequence alignment demonstrates strong conservation of the altered amino-acid residues across evolution (bottom panel); asterisks (\*) mark fully conserved positions. UniProt identifiers are given for the studied species. (D) Three-dimensional models of the *ATP5F1A* protein, highlighting the affected amino-acid positions, which are located in close proximity to the contact region between the alpha and beta subunits; by impairing local bonding interactions, the variants may alter *ATP5F1A*'s native structure, thus perturbing the formation of the inter-subunit-communication space of the ATPase complex. (E) Enzymatic analysis of OXPHOS complexes and citrate synthase in muscle tissue of Patient 5 shows a decrease in ATPase activity (complex V) relative to internal healthy controls (Salzburg, Austria). Thirty-seven independent muscle control samples were used to define the reference range; additional experimental details and the full enzymatic testing results can be found in the Supplementary online data, Table S2. OXPHOS = oxidative phosphorylation.



diagnosed with cerebral palsy<sup>18</sup> and found to be heterozygous for c.1037C > T (p.Ser346Phe); she had psychomotor retardation, spastic tetraparesis, generalized dystonia, absent speech, swallowing problems, and increased blood lactate concentrations.<sup>18</sup> None of the observed variants were present in gnomAD or in-house control databases and in silico prediction of the variants suggested their likely deleterious nature (Table). All affected amino acids exhibited a high degree of phylogenetic conservation, implying that these residues would react sensitively if altered (Fig 4C). Additionally, gnomAD indicated a selection against coding variation in *ATP5F1A* (missense- $\alpha$  and

pLI scores of 2.44 and 1.0, respectively).<sup>33</sup> Three-dimensional modeling of the mutated residues allowed us to predict the spatial distribution of the variants relative to functionally relevant sites; the variants mapped to loop regions and complex structures stabilized by multiple invariant residues close to the alpha/beta intersubunit contact area, compatible with a potential impact on protein multimerization and/or overall functionality of the ATPase complex (Fig 4D). These predictions were validated by enzymatic investigations of muscle tissue from one individual (Patient 5), showing a relevant decrease in ATPase activity (Fig 4E).

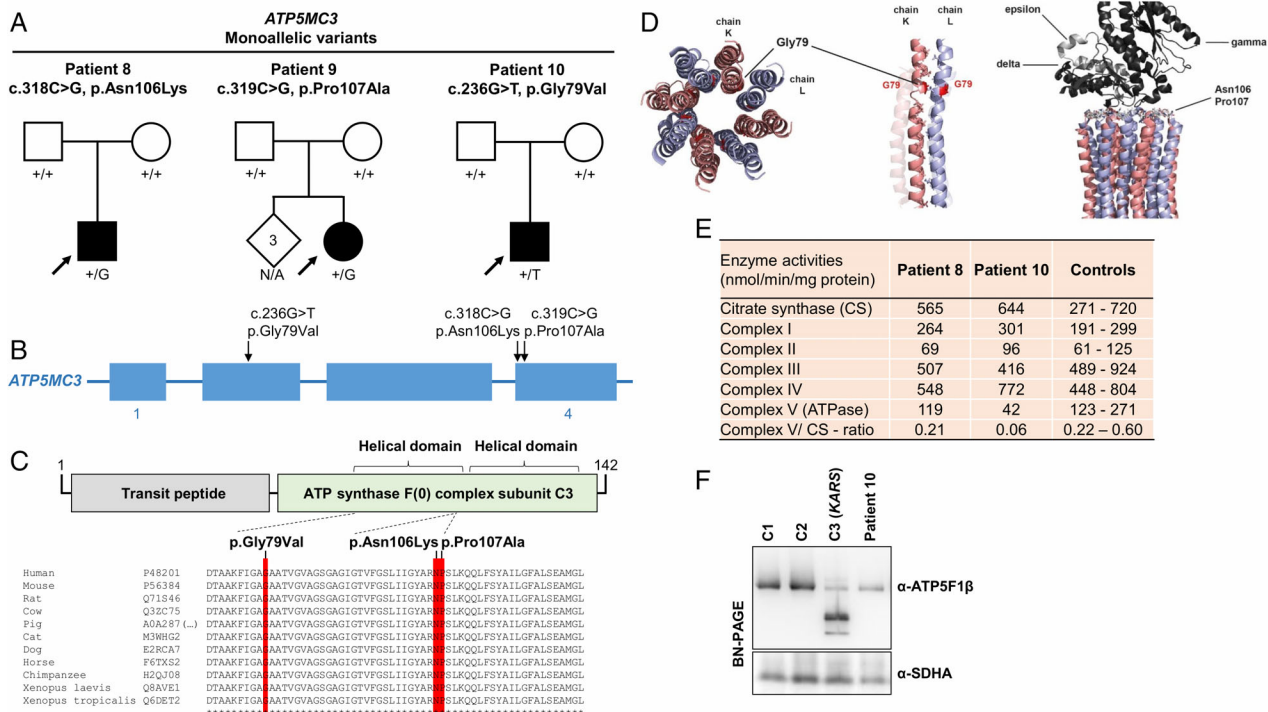


**FIGURE 5:** De novo monoallelic *ATP5MC3* variants identified in 3 cases. (A) Pedigree drawings for 3 families with heterozygous de novo variants in *ATP5MC3*. N/A, no genotyping available. (B) Exon-intron structure of *ATP5MC3* (not drawn to exact scale) with indication of the localizations of identified mutations. (C) Schematic overview of the *ATP5MC3* protein, its domain organization (boundaries are based on UniProt entry P48201), and the protein variants. A multispecies sequence alignment demonstrates strong conservation of the altered amino-acid residues across evolution (*bottom panel*); asterisks (\*) mark fully conserved positions. UniProt identifiers are given for the studied species. (D) Three-dimensional structural modeling illustrates that the mutated amino acids map to protein interaction interfaces. Gly79 lies between 2 helices, connected to each other by mostly small hydrophobic residues; p.Gly79Val may disturb this interaction by introducing a larger, less hydrophobic side-chain, thus interfering with the integrity of the c-ring structure. Asn106 and Pro107 are localized at the F<sub>0</sub>-F<sub>1</sub>-subcomplex interaction site, suggesting that mutations involving these invariant positions may translate into compromised ATPase function. (E) Enzymatic analyses of OXPHOS complexes and citrate synthase in fibroblasts of Patients 8 and 10 show a decrease in ATPase activity (complex V) as well as the complex V-citrate synthase-ratio relative to internal healthy controls (Angers, France). One hundred independent fibroblast control samples were used to define the reference range; additional experimental details and the full enzymatic testing results can be found in the Supplementary online data, Table S3. (f) BN-PAGE indicating reduced levels of ATPase in Patient 10 relative to 2 different healthy control subjects (C1 and C2); a positive control line (C3) with pathogenic KARS mutations (OMIM: 601421) resulting in profoundly aberrant ATPase assembly was also included. The experiment was performed with analysis of 6 different healthy control lines (Supplementary Fig S2) and repeated twice with similar results. Normalization of ATPase holoenzyme expression to the expression of complex II (SDHA) showed a significant decrease in ATPase protein amounts in the patient (<2 SD from mean control value); quantifications of immunoblot band intensities can be found in the Supplementary online data, Figure S2. BN-PAGE = blue native gel electrophoresis; OXPHOS = oxidative phosphorylation.

**ATP5MC3 Variants**

De novo monoallelic *ATP5MC3* missense variants were prioritized in 3 individuals (Patients 8, 9, and 10; Figs 5A, B). The first individual (Patient 8), heterozygous for c.318C > G (p.Asn106Lys), was a previously reported<sup>8</sup> 12-year-old boy who manifested isolated upper-limb dystonia. A c.319C > G (p.Pro107Ala) variant was found in the second individual (Patient 9); this 15-year-old girl had a history of milestone delay, pyramidal signs, and generalized dystonia with prominent upper-body involvement. The third individual (Patient 10) had the variant c.236G > T (p.Gly79Val); this 6-year-old boy displayed delayed psychomotor development, lower-extremity spasticity, and elevated blood lactate levels. The de novo variants were not reported in either gnomAD or local control-exome databases. In silico prediction programs consistently indicated that each variant would likely be deleterious (see Table). Although statistical models do not place *ATP5MC3* among the genes with highest mutational constraint,<sup>33</sup> the observed positions of the variants appeared to be nonrandom. All substitutions affected stringently conserved amino-acid residues located in close proximity within the carboxy-terminal helical motifs of the protein (Fig 5C); 2 variants occurred at directly neighboring nucleotides. From 3-dimensional analyses, we observed that p.Gly79Val was positioned at an interhelical contact side, whereas the other modeled variants were situated in immediate vicinity of a loop structure essentially involved in the interaction between the F<sub>O</sub> and F<sub>1</sub> sub-complexes (Fig 5D). Additional molecular features of c.318C > G (p.Asn106Lys), identified in Patient 8 and in an independent pedigree with 18 of 40 related members affected by dystonia and/or spasticity, have been described recently.<sup>8</sup> All prioritized substitutions were expected to interfere with normal ATPase structure and/or function (Fig 5D). In line with this conjecture, enzyme assays performed on Patient 10's fibroblasts identified a deficient ATPase activity (Fig 5E); this enzymatic defect was associated with a moderate decrease in assembled ATPase, as demonstrated by BN-PAGE (Fig 5F). Extending our previous characterization of Patient 8,<sup>8</sup> we also studied this individual's newly established fibroblast cultures and found that c.318C > G (p.Asn106Lys) produced a slight, but significant decrease in ATPase activity in this subject (see Fig 5E). Additionally, Patient 8's OCR was reduced (Supplementary Fig S1).

**Discussion**

Mutational lesions of nuclear genes coding for ATPase have been understudied, leading us to hypothesize that additional variation involving these loci might be

etiologically related to clinical phenotypes. We tested this hypothesis by analyzing WES-derived rare-variant collections of patients with suspected mitochondrial disorders and/or dystonia, resulting in the prioritization of alleles with strong evidence for disease causality in *ATP5F1E*, *ATP5PO*, *ATP5F1A*, and *ATP5MC3*. Independent support for these discoveries was generated through international collaborations facilitated by GeneMatcher, which led to the identification of additional cases with likely disease-relevant variants in three of these genes. Our investigation provides a rare insight into the genetic and clinical spectrum of under-recognized ATPase-related neurologic conditions. Moreover, the study represents a unique cohort-based analysis, also implementing the interrogation of a large set of parent-affected child trio sequencing data (15% of the 2,962 index presentations in the initial-analysis cohorts).

First, we were able to replicate *ATP5F1E* as a recessive disease gene in 3 unrelated patients, all of whom shared an identical homozygous variant. Using immunohistochemical staining in different cell types, we confirmed previous results showing marked reduction of intact ATPase complex in association to the *ATP5F1E* recurrent mutation.<sup>9</sup> Second, we identified and functionally validated compound-heterozygous variants in *ATP5PO*, a gene not previously implicated in monogenic disease. We used RNA-seq, proteomics, and immunoblotting approaches based on the patient's fibroblasts to demonstrate that the variants were loss-of-function alterations resulting in diminished amounts of ATPase. Third, our study allowed us to define an unexpected role for de novo dominant mutations at 2 loci: *ATP5F1A*, which has only been linked to recessive conditions until now<sup>10,11</sup>; and *ATP5MC3*, for which a disease association has yet been based on the identification of only a single mutant genotype.<sup>8</sup> An array of bioinformatics, populational, and experimental data supported our contention that the observed de novo variants were causative for the phenotypes: (1) the mutated amino-acid sites were invariant across species; (2) the variants were present neither in gnomAD nor in any other available control database; (3) in silico tools based on protein sequence and amino-acid structure predicted pathogenicity; (4) molecular modeling analyses suggested detrimental effects for each variant; and (5) findings from enzymatic studies performed in fibroblasts from cases with *ATP5F1A* c.620G > A, *ATP5MC3* c.236G > T, and *ATP5MC3* c.318C > G were consistent with ATPase defects. Although we could not be certain about the disease-causing character of each de novo change that we found, we noted that all these variants met criteria for classification as likely pathogenic/pathogenic according to American College of Medical Genetics &

Genomics (ACMG) guidelines (see Table).<sup>34</sup> Because ACMG classifications should be treated with caution in the context of new gene-phenotype associations,<sup>34</sup> we stress that some de novo variants lack a clear proof of pathogenicity. Nevertheless, in support of the variants' disease-relevance, 2 of the identified *ATP5F1A* alleles turned out to be recurrent among human disease-subjects: c.620G > A was found to be listed as an independent de novo hit in association with lactic acidosis in ClinVar (accession VCV000432972.3),<sup>35</sup> whereas c.545G > A was seen as 2 separate occurrences in a published catalogue of candidate neurodevelopmental disorder-associated de novo variants.<sup>36</sup> Additionally, based on the recurrence of c.318C > G found in one individual from our herein studied dystonia cohort (referred to here as Patient 8; and as "proband/family-2" in Neilson et al<sup>8</sup>) and in an independent multigenerational pedigree, *ATP5MC3* has already been suggested as a candidate gene for autosomal-dominant phenotypes.<sup>8</sup> In the independent pedigree,<sup>8</sup> c.318C > G was detected among 18 individuals with variable dystonia-spasticity presentations, 2 of whom were demonstrated to exhibit mild cellular ATPase defects. These examples of variant recurrence provide strong arguments in favor of the implication of *ATP5F1A* and *ATP5MC3* in our patients' phenotypes. At the same time, with the identification of non-recurrent de novo hits, especially c.236G > T for which functional data are provided, our present study enlarges the spectrum of disease-associated genotypes for *ATP5MC3* and consolidates its link to disease.

In our populations of individuals with suspected mitochondrial pathologies and dystonia, we estimate the frequencies of phenotypes related to mutations in nuclear ATPase-encoding genes at 0.3% (5/1,950) and 0.2% (2/1,012), respectively; this information may prove useful for the design of future genetic testing and clinical trial approaches.

The core function of ATPase is synthesizing the main bulk of cytosolic ATP.<sup>2</sup> ATP demands vary between developmental stages and tissues.<sup>4</sup> An especially tight regulation of ATP production is required within the central nervous system, as evidenced by the vulnerability of this organ in diverse mitochondrial dysfunction syndromes.<sup>37</sup> Complete loss of human ATPase is likely incompatible with life<sup>4</sup>; changes in the abundance of ATPase or its functionality, however, have been shown to result in clinical disease.<sup>6,7</sup> In model organisms, both loss- and gain-of-function point mutations affecting ATPase subunits have been associated with cellular pathology.<sup>38</sup> Although the molecular consequences of the herein reported variants remain to be further elucidated, we speculate that differences in (residual) ATPase activities may account for the

phenotypic variability observed in our series. The majority of patients had movement disorders (8/10) and neurodevelopmental abnormalities (9/10), including developmental delay and varying levels of intellectual disability. Consistent with impairments of the OXPHOS system,<sup>5</sup> lactate concentrations were elevated in blood and/or CSF of 7 patients. Four patients exhibited pyramidal signs or spasticity. Of the patients with available brain MRIs (9/10), one demonstrated global atrophy (*ATP5PO*) and 3 had (mostly unspecific) signal alterations (*ATP5F1E*, *ATP5F1A*, and *ATP5MC3*); images were nondiagnostic in most cases with dystonia-predominant phenotypes (Patients 2, 6, 7, 8, and 9) and observed abnormalities showed no consistent phenotype. Disease severity was remarkably heterogeneous. The severest course was evident in Patient 4 with *ATP5PO* mutations, who presented with intractable epilepsy, neurodegeneration, and early death. Based on our functional studies, it is likely that Patient 4 suffered from profound ATPase impairments leading to rapid clinical decline. Neonatal life-threatening metabolic deterioration, medication-refractory movement abnormalities, and respiratory failure were presented by individuals with the *ATP5F1E* mutation, although stabilized disease courses were observed at an older age; the severe findings for pediatric individuals may also relate to profoundly disrupted ATPase functions, as indicated by our cellular investigations. Comparatively milder manifestations were seen in association to *ATP5F1A* and *ATP5MC3* variants, ranging from metabolic abnormalities with spontaneous resolution to extrapyramidal/pyramidal signs with variable neurodevelopmental comorbidity. When analyzing our *ATP5MC3*-mutated subjects together with available data from the multigenerational family reported by Neilson et al (15 individuals with clinical information),<sup>8</sup> features of the *ATP5MC3*-associated condition include dystonia (12/18), spasticity/pyramidal signs (17/18), and developmental delay/intellectual disability (2/18). Dystonia-predominant syndromes were documented in 10 individuals (Patients 8 and 9; and 8 subjects from the multigenerational family<sup>8</sup>). Notably, our description of the previously unreported Patients 9 and 10 confirms the manifestation of spastic symptoms in independent families with *ATP5MC3* variants, and newly introduces the expression of neurodevelopmental comorbidity. Our study thus allows to define a relevant degree of phenotypic differences between unrelated *ATP5MC3*-mutated families. The mechanisms through which *ATP5F1A* and *ATP5MC3* variants cause disease remain incompletely understood. Dominant-negative effects could well be possible, as supported by the observation of mild-to-moderate ATPase assembly and/or enzyme-activity defects in several patient lines. Notably, our experiments

performed for Patients 8 and 10 revealed that *ATP5MC3* c.236G > T, associated with a more severe neurodevelopmental disease-spasticity presentation, produced a significantly greater ATPase enzyme deficit than *ATP5MC3* c.318C > G, associated with isolated dystonia. However, further studies are required before genotype–phenotype correlations can be clearly postulated. Dystonia – including isolated (1/10) and complex (6/10) dystonia – was a cardinal symptom in our series, although an ascertainment bias introduced by the interrogation of a large dystonic cohort may have contributed to this predominance. Non-neurologic abnormalities involving the heart, kidneys, and liver were also observed in our series, and such features may be more prominent when screening other patient cohorts for ATPase defects. We also emphasize that a considerable subset of mitochondriopathy-related genes has already been associated with dystonia and other movement disorders,<sup>39</sup> highlighting that such presentations should not be considered pathognomonic for ATPase-related diseases.

The observed occurrence of both biallelic<sup>10,11</sup> and de novo monoallelic mutations in one of the herein described disease genes, *ATP5F1A*, is intriguing. In the group of mitochondrial disorders, different inheritance characteristics of causative variants within the same gene have rarely been reported.<sup>5,37</sup> Moreover, most monogenic forms of mitochondrial disease elucidated to date have been associated with autosomal-recessive patterns of inheritance.<sup>5,37</sup> It remains to be seen whether de novo mutations and/or dual modes of variant inheritance represent broader characteristics of disease causation in mitochondrial disorders. We anticipate that de novo variants in mitochondrial disorders are likely underdiagnosed given that larger-scale sequencing studies in the field have not systematically used trio analysis designs.<sup>39</sup>

In summary, we describe a series of 10 individuals with likely disease-causing variants in different subunits of mitochondrial ATPase and provide evidence that mutations of this complex can act through either a biallelic or monoallelic mechanism. The associated phenotypes were heterogeneous but combined similar features including neurodevelopmental issues, movement disorders, and elevated lactate concentrations. Our study illustrates that large patient collections and family based sequencing designs will be instrumental in defining new genotype–phenotype relationships in the field of mitochondrial disorders.

---

## Acknowledgments

The authors would like to thank the patients and their families who took part in our study. This study was

funded in part by a research grant from the Else Kröner-Fresenius-Stiftung as well as by in-house institutional funding from Technische Universität München, Munich, Germany, Helmholtz Zentrum München, Munich, Germany, Medizinische Universität Innsbruck, Innsbruck, Austria, and Charles University, Prague, Czech Republic (PROGRES Q27). This study was also funded by the Czech Ministry of Education under grant AZV: NV19-04-00233 and under the frame of EJP RD, the European Joint Programme on Rare Diseases (EJP RD COFUND-EJP No. 825575). M.Z. and J.W. receive research support from the German Research Foundation (DFG 458949627; ZE 1213/2-1; WI 1820/14-1). S.B. is a member of the European Reference Network for Rare Neurological Diseases – Project ID No. 739510. M.C.K. has received funding from the U.S. National Institute of Neurological Disorders & Stroke 1R01 NS106298. Analysis of Patient 7 was provided by the Broad Institute of MIT and Harvard Center for Mendelian Genomics (Broad CMG) and was funded by the National Human Genome Research Institute grants UM1 HG008900 (with additional support from the National Eye Institute, and the National Heart, Lung and Blood Institute), U01 HG0011755, and R01 HG009141 and in part by grant number 2020-224274 from the Chan Zuckerberg Initiative DAF, an advised fund of Silicon Valley Community Foundation. F.D. receives research support from the German Research Foundation (DI 1731/2-2) and was supported by a grant from the “Elterninitiative Kinderkrebsklinik e.V.” (Düsseldorf; #701900167). The authors acknowledge support by the German Federal Ministry of Education and Research (BMBF, Bonn, Germany) awarded grant to the German Network for Mitochondrial Disorders (mitoNET, 01GM1906A), the German BMBF, the Austrian Science Funds (FWF), and Horizon2020 through the E-Rare project GENOMIT (01GM1920A, I4695-B, genomit.eu), and the ERA PerMed project PerMiM (01KU2016A, I4704-B, permim.eu). We gratefully thank Jennifer Alban and Justine Faure (Angers, France) for their generous contribution with enzyme activity and immunoblotting analyses. Open Access funding enabled and organized by Projekt DEAL.

## Author Contributions

M.Z., R.K., K.S., R.S., J.W., and H.P. contributed to study concept and design. All authors contributed to data acquisition and analysis. M.Z., R.K., K.S., C.B., N.G., R. G.F., and M.T.A. contributed to drafting the manuscript and figures.

## Potential Conflicts of Interest

None of the authors has any relevant conflict of interest to declare.

## References

- Gorman GS, Chinnery PF, DiMauro S, et al. Mitochondrial diseases. *Nat Rev Dis Primers* 2016;2:16080.
- Yoshida M, Muneyuki E, Hisabori T. ATP synthase—a marvellous rotary engine of the cell. *Nat Rev Mol Cell Biol* 2001;2:669–677.
- He J, Ford HC, Carroll J, et al. Assembly of the membrane domain of ATP synthase in human mitochondria. *Proc Natl Acad Sci U S A* 2018;115:2988–2993.
- Jonckheere AI, Smeitink JA, Rodenburg RJ. Mitochondrial ATP synthase: architecture, function and pathology. *J Inher Metab Dis* 2012;35:211–225.
- Schlieben LD, Prokisch H. The dimensions of primary mitochondrial disorders. *Front Cell Dev Biol* 2020;8:600079.
- Galber C, Carissimi S, Baracca A, Giorgio V. The ATP synthase deficiency in human diseases. *Life (Basel)* 2021;11:325. <https://doi.org/10.3390/life11040325>
- Dautant A, Meier T, Hahn A, et al. ATP synthase diseases of mitochondrial genetic origin. *Front Physiol* 2018;9:329.
- Neilson DE, Zech M, Hufnagel RB, et al. A novel variant of ATP5MC3 associated with both dystonia and spastic paraplegia. *Mov Disord* 2021 (Online ahead of print). <https://doi.org/10.1002/mds.28821>.
- Mayr JA, Havlickova V, Zimmermann F, et al. Mitochondrial ATP synthase deficiency due to a mutation in the ATP5E gene for the F1 epsilon subunit. *Hum Mol Genet* 2010;19:3430–3439.
- Jonckheere AI, Renkema GH, Bras M, et al. A complex V ATP5A1 defect causes fatal neonatal mitochondrial encephalopathy. *Brain* 2013;136:1544–1554.
- Lieber DS, Calvo SE, Shanahan K, et al. Targeted exome sequencing of suspected mitochondrial disorders. *Neurology* 2013;80:1762–1770.
- Olahova M, Yoon WH, Thompson K, et al. Biallelic mutations in ATP5F1D, which encodes a subunit of ATP synthase, cause a metabolic disorder. *Am J Hum Genet* 2018;102:494–504.
- Barca E, Ganetzky RD, Potluri P, et al. USMG5 Ashkenazi Jewish founder mutation impairs mitochondrial complex V dimerization and ATP synthesis. *Hum Mol Genet* 2018;27:3305–3312.
- Stenton SL, Shimura M, Piekutowska-Abramczuk D, et al. Diagnosing pediatric mitochondrial disease: lessons from 2,000 exomes. *medRxiv* [Preprint]. <https://doi.org/10.1101/2021.06.21.21259171>.
- Zech M, Jech R, Boesch S, et al. Monogenic variants in dystonia: an exome-wide sequencing study. *Lancet Neurol* 2020;19:908–918.
- Sobreira N, Schiettecatte F, Valle D, Hamosh A. GeneMatcher: a matching tool for connecting investigators with an interest in the same gene. *Hum Mutat* 2015;36:928–930.
- Duzkale N, Oz O, Turkmenoglu TT, et al. Investigation of hereditary cancer predisposition genes of patients with colorectal cancer: single-Centre experience. *J Coll Physicians Surg Pak* 2021;30:811–816.
- Jin SC, Lewis SA, Bakhtiari S, et al. Mutations disrupting neuritogenesis genes confer risk for cerebral palsy. *Nat Genet* 2020;52:1046–1056.
- Ziegler A, Bader P, McWalter K, et al. Confirmation that variants in TT12 are responsible for autosomal recessive intellectual disability. *Clin Genet* 2019;96:354–358.
- The UniProt C. UniProt: the universal protein knowledgebase. *Nucleic Acids Res* 2017;45:D158–D169.
- Sievers F, Wilm A, Dineen D, et al. Fast, scalable generation of high-quality protein multiple sequence alignments using Clustal omega. *Mol Syst Biol* 2011;11:539.
- Ng PC, Henikoff S. Predicting deleterious amino acid substitutions. *Genome Res* 2001;11:863–874.
- Adzhubei IA, Schmidt S, Peshkin L, et al. A method and server for predicting damaging missense mutations. *Nat Methods* 2010;7:248–249.
- Kircher M, Witten DM, Jain P, et al. A general framework for estimating the relative pathogenicity of human genetic variants. *Nat Genet* 2014;46:310–315.
- Berman HM, Westbrook J, Feng Z, et al. The Protein Data Bank. *Nucleic Acids Res* 2000;28:235–242.
- Feichtinger RG, Olahova M, Kishita Y, et al. Biallelic C1QBP mutations cause severe neonatal-, childhood-, or later-onset cardiomyopathy associated with combined respiratory-chain deficiencies. *Am J Hum Genet* 2017;101:525–538.
- Charif M, Gueguen N, Ferre M, et al. Dominant ACO2 mutations are a frequent cause of isolated optic atrophy. *Brain Commun* 2021;3:fcab063.
- Kremer LS, Bader DM, Mertes C, et al. Genetic diagnosis of Mendelian disorders via RNA sequencing. *Nat Commun* 2017;8:15824.
- Invernizzi F, Legati A, Nasca A, et al. Myopathic mitochondrial DNA depletion syndrome associated with biallelic variants in LIG3. *Brain* 2021;144:e74.
- Kopajtic R, Smirnov D, Stenton SL, et al. Integration of proteomics with genomics and transcriptomics increases the diagnostic rate of Mendelian disorders. *bioRxiv* [Preprint]. <https://doi.org/10.1101/2021.03.09.21253187>.
- Ritchie ME, Phipson B, Wu D, et al. Limma powers differential expression analyses for RNA-sequencing and microarray studies. *Nucleic Acids Res* 2015;43:e47.
- Gueguen N, Piarroux J, Sarzi E, et al. Optic neuropathy linked to ACAD9 pathogenic variants: a potentially riboflavin-responsive disorder? *Mitochondrion* 2021;59:169–174.
- Karczewski KJ, Francioli LC, Tiao G, et al. The mutational constraint spectrum quantified from variation in 141,456 humans. *Nature* 2020;581:434–443.
- Richards S, Aziz N, Bale S, et al. Standards and guidelines for the interpretation of sequence variants: a joint consensus recommendation of the American College of Medical Genetics and Genomics and the Association for Molecular Pathology. *Genet Med* 2015;17:405–424.
- Landrum MJ, Lee JM, Benson M, et al. ClinVar: public archive of interpretations of clinically relevant variants. *Nucleic Acids Res* 2016;44:D862–D868.
- Kaplanis J, Samocha KE, Wiel L, et al. Evidence for 28 genetic disorders discovered by combining healthcare and research data. *Nature* 2020;586:757–762.
- Gusic M, Prokisch H. Genetic basis of mitochondrial diseases. *FEBS Lett* 2021;595:1132–1158.
- Kucharczyk R, Zick M, Bietenhader M, et al. Mitochondrial ATP synthase disorders: molecular mechanisms and the quest for curative therapeutic approaches. *Biochim Biophys Acta* 2009;1793:186–199.
- Stenton SL, Prokisch H. Genetics of mitochondrial diseases: identifying mutations to help diagnosis. *EBioMedicine* 2020;56:102784.